

# Structural and Electronic Properties of Doped Silicon Nanowire

Anurag Srivastava<sup>1</sup>, Florina Regius<sup>2</sup>

<sup>1,2</sup>Advance Materials Research Lab, Indian Institute of Information Technology and Management, Gwalior, Madhya Pradesh, India

**Abstract:** *Electronic and structural properties of Silicon Nanowire (SiNW) when doped with Al and P atoms are obtained from simulation studies have been reviewed. The bandgap, density of states and Structural property of Silicon Nanowire has been compared when this nanowire is doped with phosphorous and aluminium atoms. We observed that decrease in bandgap increases the metallic property of silicon. Total energy is maximum then the structure is least stable. So we can say that total energy is inversely proportional to stability. In density of states, we clearly see the decline in DOS/Ev with the increase of doping Al and P atoms. In this paper, we have discussed all the electronic and structural properties.*

**Keywords:** Band structure, Band gap, Density of States, SiNW, Aluminium

## 1. Introduction

The nanowire, a structure that has an amazing length-to-width ratio. Nanowires can be incredibly thin -- it's possible to create a nanowire with the diameter of just one nanometre, though engineers and scientists tend to work with nanowires that are between 30 and 60 nanometres wide. Scientists hope that we will soon be able to use nanowires to create the smallest transistors yet, though there are some pretty tough obstacles in the way. Nanowires possess unique electrical, electronic, thermo electrical, optical, magnetic and chemical properties, which are different from that of their parent counterpart. Silicon NW is the answers for ongoing obstacles in electronic field. This Si NW is the one-dimensional structures. Their electronic conduction can be controlled by doping. Si NW can be used from field effect transistor to Biosensors.[4,5] The photoluminescence in Si NW and nanoparticle have been observed [7,8] which is an experimental evidence of the quantum confinement.[ 6] Silicon-wire research started in the mid 1990s, when advances in microelectronics triggered a renewed interest in silicon—now nanowire—research. [1] Last, we will turn our attention to the electrical properties of silicon nanowires and discuss the different doping methods. Then, three effects essential for the conductivity of a silicon nanowire are treated. [9] Experimentally it has been observed that the band Gap can be tuned by choosing different growth directions and diameters of wire. [10] The electronic structure of Si NW being critically depends on the size, orientation; passivation and doping level of nanostructure. These are the diameter dependence of the dopant ionization efficiency, the influence of surface traps on the charge-carrier density, also causing a diameter dependence, and the charge-carrier mobility in silicon nanowires. [1] Many techniques, including both top-down and bottom-up approaches, have been developed and applied for the synthesis of Nanowires. Vapor-Liquid-Solid (VLS) Mechanism, Chemical Vapor Deposition (CVD), Evaporation of SiO, Molecular Beam Epitaxy (MBE), Laser Ablation and Electroless metal deposition and dissolution (EMD) [2]. These days Si NW are used for enhanced thermo electric performance [3]. Silicon nanowire can be uniformly made at low temperature using Vapour-Liquid-Solid growth.

## 2. Computational Method

We have performed the calculation using the ab-initio pseudopotential method which is based on the density functional theory and analyse the electronic properties of silicon nanowire (alpha). We have used atomix toolkit (ATK)[11] for computation, a further development of TranSIESTA-C[13,14] which, in turn, is based on the technology, models and algorithms developed in the academic code TranSIESTA and, in part, McDCal [12], employing localized basis sets as developed in SIESTA[15]. The computation has been made in self-consistent manner using steepest descent geometric optimization with Pulay Algorithm for iteration mixing. A mesh cut-off of 70 Hartree has been used throughout the study. The Brillouin-zone (BZ) integration is performed with a Monkhorst-Pack scheme using 1\*1\*11 k points. The cutoff energy and the number of k points are varied to test the convergence and are found to converge within the force tolerance of 0.05eV/A for the reported value. The exchange correlation functional described within the extended huckel and with generalised gradient approximation revised-PBE (rev-PBE) as proposed by Zhang and Yang [16] are used for the computation of total energies of Si Nanowire and its doping with aluminium and phosphorous atoms. The total energy for Si nanowire extended huckel potential is -2426.37 eV. The extended huckel potential is quite good for the computation of total energy.[17] The nanowires are placed in the supercell along the wire length in z-direction while the supercell lengths in the x and y direction are chosen big enough to avoid interaction between nanowire and its periodic image.[18] For better understanding of fundamental physics associated with different structures, the binding energies of Si nanowire have also been analysed and to understand the nature of material, localization and delocalization of states near the Fermi level, we have analysed the electronic band structure and density of states for all the doping configuration of Si nanowire.

### 3. Results

#### 3.1 Structural Properties

The atomic configurations of the Si Nanowire are presented in the Fig 1. It may be cautioned that these figures are schematic and separations between atoms are not to scale. As these figures depicts the structures quite clearly and hence have not been discussed separately in the text. The stability energetic in the various nanostructures of Si has been performed under the extended huckel with the revised PBE type exchange correlation functional and shown in Fig.2 by total energy per atom for all the Si nanowire structure have been reported in Table 1. We observe that silicon nanowire has the lowest energy is visible at -2426.37 ev which shows it is the most stable structure and when it is doped with one aluminium atom the total energy is -2375.27 ev which is less lower than earlier which shows it is next stable structure. In this way total energy increases with the increase of doping of Aluminium atoms in Si nanowire. Now after doping with phosphorous atoms, the total energy has a great variation. --2468.46 ev is the lowest energy found when Sillicon nanowire is doped with the four phosphorous atoms. This shows it is highly stable structure. - 2510.69 ev is the next lower energy found when Sillicon nanowire is doped with the three phosphorous atoms. It is also highly stable but lesser then earlier. Here, we observe that with increase in doping of atoms, total energy decreases and stability increases. Now for detail of structural stability, the formation energy and binding energy are calculated. [19]

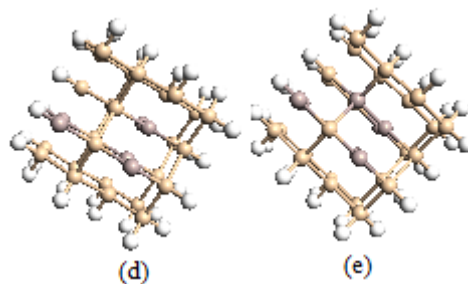
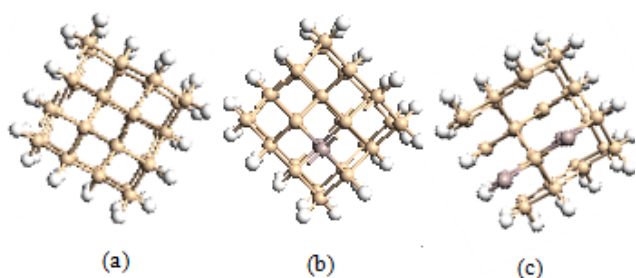
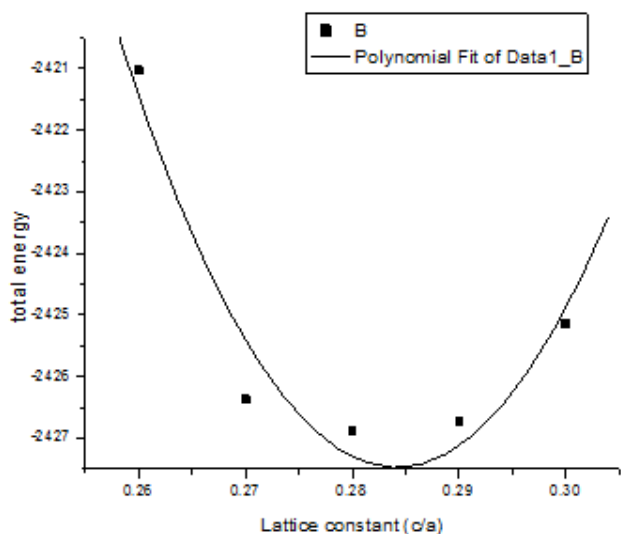


**Figure 2:**The atomic Configurations of Si nanowires (a) SiNW without doping , (b) SiNW doped with 1 Al atom , (c) SiNW doped with 2 Al atoms , (d) SiNW doped with 3 Al atoms and (e) SiNW Doped with 4 Al atoms

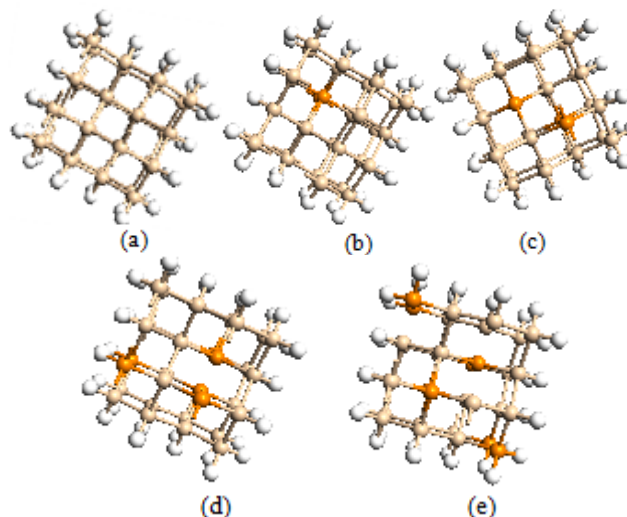


**Figure 3:**The atomic Configurations of Si nanowires (a) SiNW without doping , (b) SiNW doped with 1 P atom , (c) SiNW doped with 2 P atoms , (d) SiNW doped with 3 P atoms and (e) SiNW Doped with 4 P atoms

**Table:**

Atomic Configuration	Lattice constant	Total energy	Binding energy	Formation energy
Silicon Pristine	0.285	-2426.37	4.29	-
Doped with 1 Al atom	0.27	-2375.27	4.64	1.29
Doped with 2 Al atoms	0.27	-2326.86	4.99	2.55
Doped with 3 Al atoms	0.29	-2282.88	5.35	3.71
Doped with 4 Al atoms	0.30	-2237.89	5.70	4.9
Doped with 1 P atom	0.27	-2468.46	3.89	0.58
Doped with 2 P atoms	0.27	-2510.69	3.49	1.66
Doped with 3 P atoms	0.27	-2548.93	3.03	1.8
Doped with 4 P atoms	0.27	-2594.44	2.88	2.33

#### 3.2 Bandstructure analysis

To understand the material behaviour of the stable geometries of Silicon Nanowires, electronic band structures analysis have been performed and their band structures are compared in Fig 3a-g . On the basis of doping atoms crossing the Fermi level, conductivity of various Si nanowires has been explained. The bandstructure of bulk Si nanowire as shown in Fig.3a. no conduction bands are crossing which shows it is semiconductor . It has a bandgap of 8.03 E/ev .When the Si nanowire is doped with 1 Al atom as shown in Fig.3b there is no band gap and two conduction line is crossing the Fermi level at 0.1 E/ev. This shows metallic property has entered the play. Now the Sillicon nanowire is doped with 2 Al atoms as shown in Fig.3c as

usual there is no band gap and two conduction lines are crossing the Fermi level at 0.01 E/ev and -0.01E/ev from valence and conduction bands resp. This shows metallic property has increased compared to previous. Then Si nanowire is doped with three Aluminium atoms as shown in Fig.3d and two conduction lines are intersecting the Fermi level at 0.1 E/ev and - 0.1 E/ev resp. Conduction band becoming dense. Metallic property has increased from earlier. Finally Si nanowire is doped by 4 Al atoms as shown in Fig.3e and even in this three conduction lines are crossing at 0.02 E/ev ,0.01and-0.0 1 E/ev resp. Conduction band has become more denser because of crowded conduction lines . Metallic property also increased. Now it is turn of Phosphorous atoms to be doped in Si nanowire. The Si nanowire is doped with 1 P atom as shown in Fig.3f. There is no band gap and a conduction line is crossing the Fermi level below -0.002 E/ev. This shows metallic property is

more in case of phosphorous. Now the Silicon nanowire is doped with two Phosphorous atoms as shown in Fig.3g as usual there is no band gap and three conduction lines are crossing the Fermi level below -1.0 E/ev , -1.2 E/ev , -0.2 E/ev resp. This shows metallic property has increased compared to previous. Then Si nanowire is doped with three P atoms as shown in Fig.3h and here also there are three conduction lines which is crossing the Fermi level from valence and conduction band has become more dense and thick compared to others. Finally Si nanowire is doped by 4 phosphorous atoms as shown in Fig.3i in which four conduction lines are intersecting the Fermi level at valence band and two conduction lines intersecting at conduction band. The graph is becoming dense to denser while increasing the number of atoms which shows the metallic nature increases.

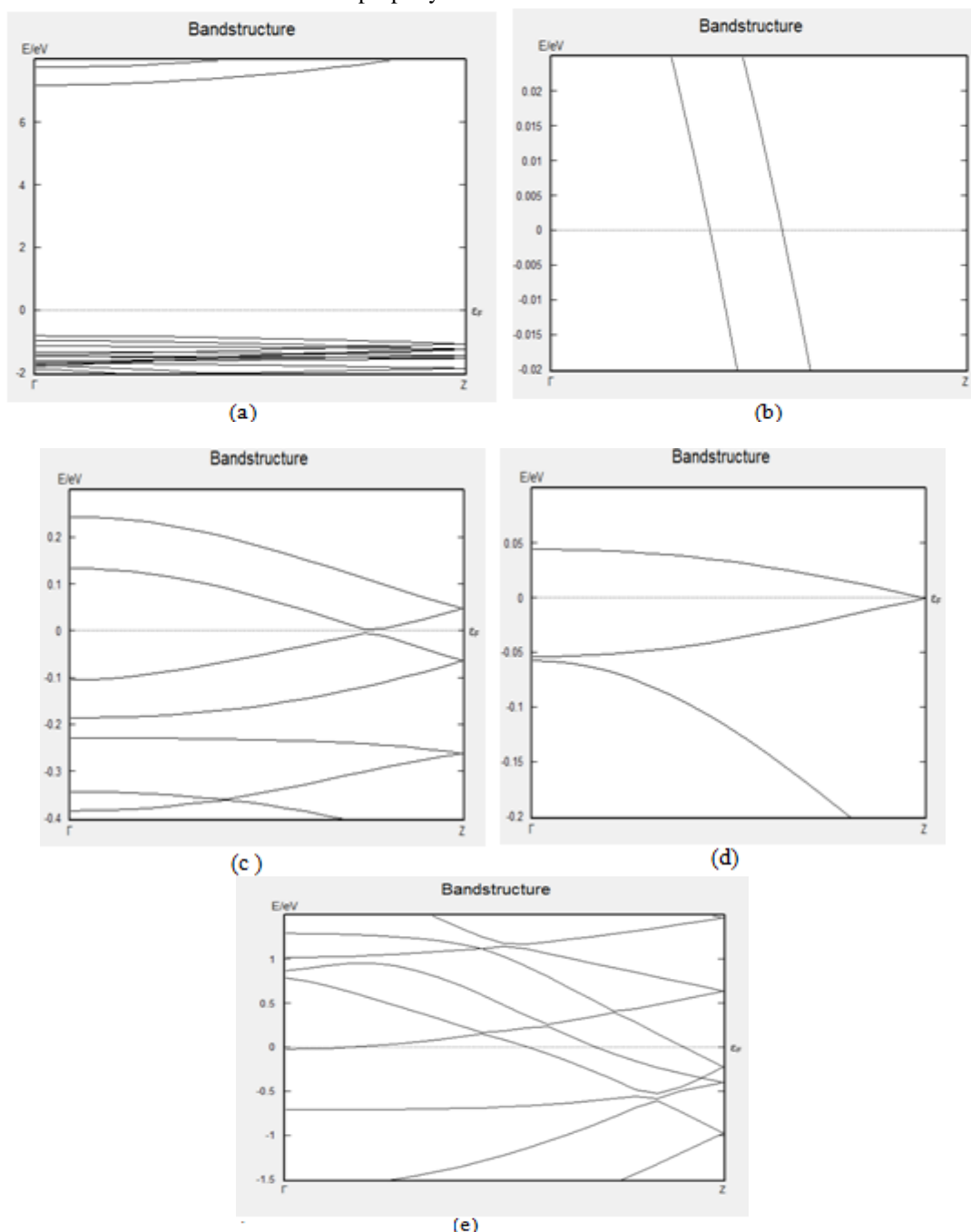


**Figure4:**The Bandstructures of Si nanowires (a) SiNW without doping , (b) SiNW doped with 1 Al atom , (c) SiNW doped with 2 Al atoms , (d) SiNW doped with 3 Al atoms and (e) SiNW Doped with 4 Al atoms

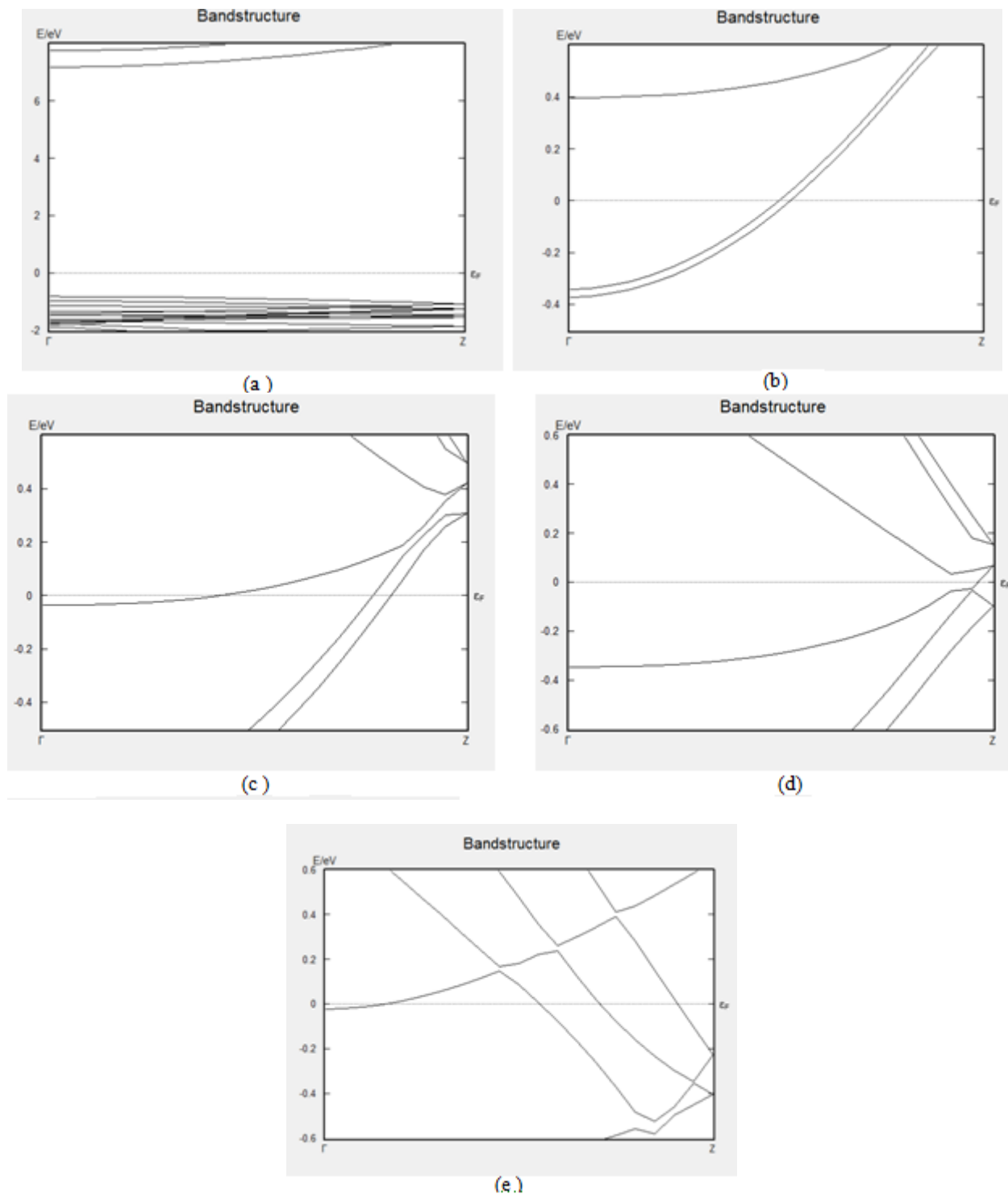


**Figure 5:** The Bandstructures of Si nanowires (a) SiNW without doping , (b) SiNW doped with 1 P atom , (c) SiNW doped with 2 P atoms , (d) SiNW doped with 3 P atoms and (e) SiNW Doped with 4 P atoms

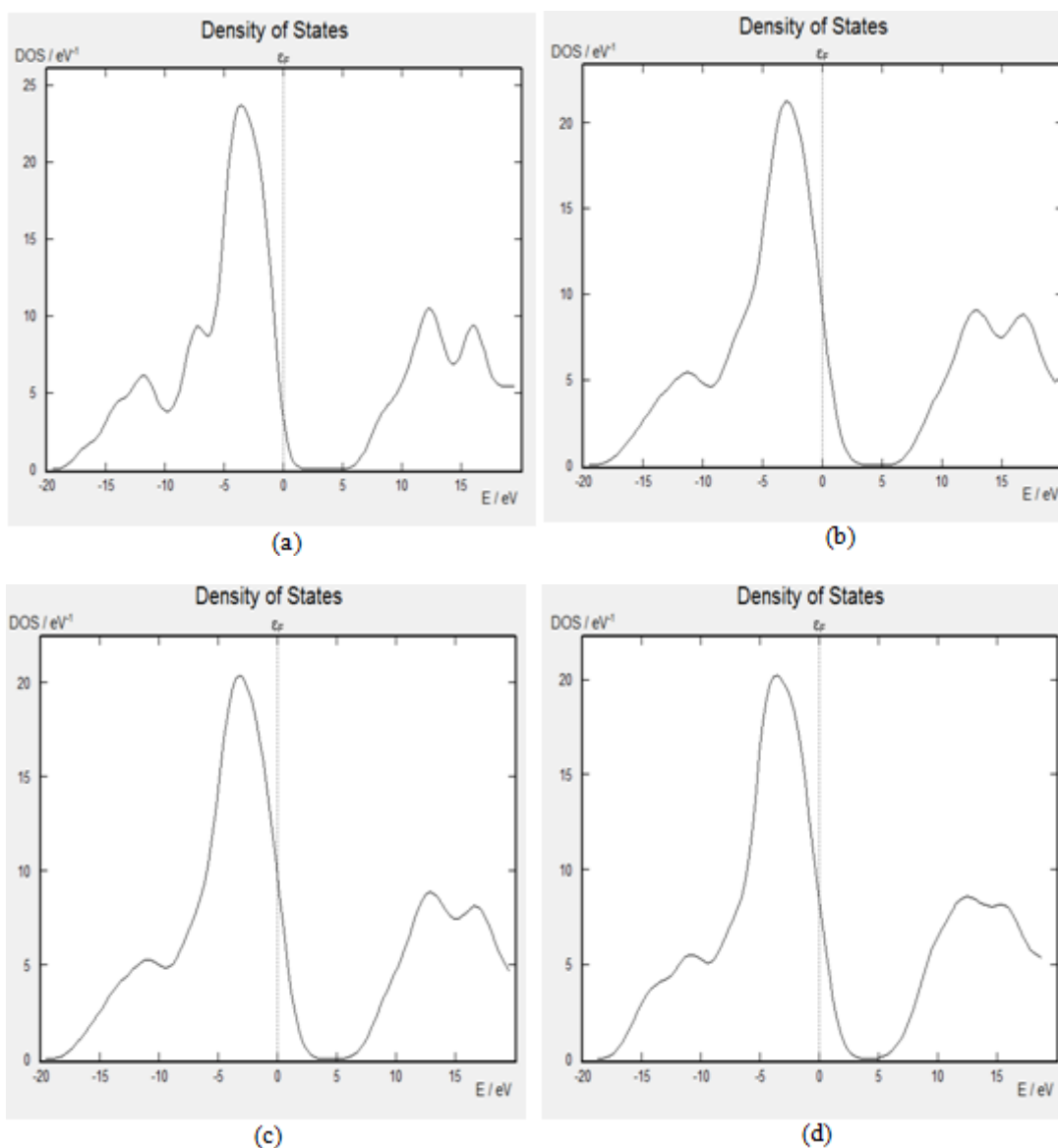
### 3.3 Density of States

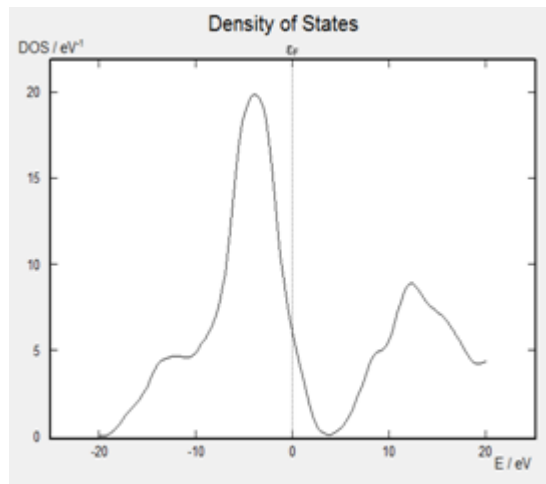
The DOS profile for all the stabilized structures have been shown in Fig 4a-g along with that of bulk Silicon . In case of bulk Silicon nanowire, the graph shows a high peak which is at 23.7 DOS/ev in y axis and -4.2 E/ev on x axis. Two peaks are present which are on the left and right side of high peak. The peak on the right side appears on 10.4, 9.4 DOS/ev on y axis resp. and 11, 15.4 E/ev in x axis resp. But the peak on the left side is present on 9.3, 6.1 DOS/ev on axis y resp and - 6, -12 E/ev in x axis. We observe a small bandgap which shows the semi conducting behaviour. When

this bulk Silicon nanowire is doped with a Al atom, the graph shows a high peak which is at 21.2 DOS/ev in y axis and -4 E/ev on x axis. There are two peaks on the right side is present on 7.3, 5.4 DOS/ev on y axis and -6.3, -11.2 E/ev in x axis. But the peak on the left side is appears on 9, 8.8 DOS/ev on axis y and -14.2, 16 E/ev in x axis. Then this bulk Silicon nanowire is doped with two Al atom, the graph shows a high peak which is at 20.4 DOS/ev in y axis and -3 E/ev on x axis. The peak on the right side is present on 11.5 DOS/ev on y axis and 5.2 E/ev in x axis. But the peak on the left side is present on 8, 8.9 DOS/ev on axis y and 14, 17 E/ev in x axis resp. We see that the peaks are diminishing

with the increase in number of Al and P atoms .Now , this bulk Sillicon nanowire is doped with three Al atom , the graph shows a high peak which is at 20.2 DOS/ev in y axis and -2.8 E/ev on x axis . There are two peaks on the right side which appears on 5.5, 4 DOS/ev on y axis resp. and -11,14 E/ev in x axis resp. But there are two peaks on the left side is present on 8.7, 8 DOS/ev on axis y and -11, 15.4 E/ev in x axis resp. And then this bulk Sillicon nanowire is doped with four Al atom , the graph shows a high peak which is at 19.4 DOS/ev in y axis and -4.7 E/ev on x axis . There are two peaks on the right side which appears on 3.7, 5.4 DOS/ev on y axis resp. and -13,-15 E/ev in x axis resp. But there are two peaks on the left side is present on 7.4, 8.2 DOS/ev on y axis and 10 , 11.7 E/ev in x axis resp. . The left side of Fermi level is denser which clearly indicates high metallic nature. Now it's the turn for phosphorous doping on Sillicon nanowire . When this bulk Sillicon nanowire is doped with a P atom, the graph shows a high peak which is at 22.67 DOS/ev in y axis and -11 E/ev on x axis. There are three peaks on the right side appears on 4.4 , 6 , 8.7 DOS/ev on y axis and -11,-17,-20.7 E/ev in x axis resp. But there are 5 peaks on the left side is present on 9.5,9.7,4.7,1.6,1.08

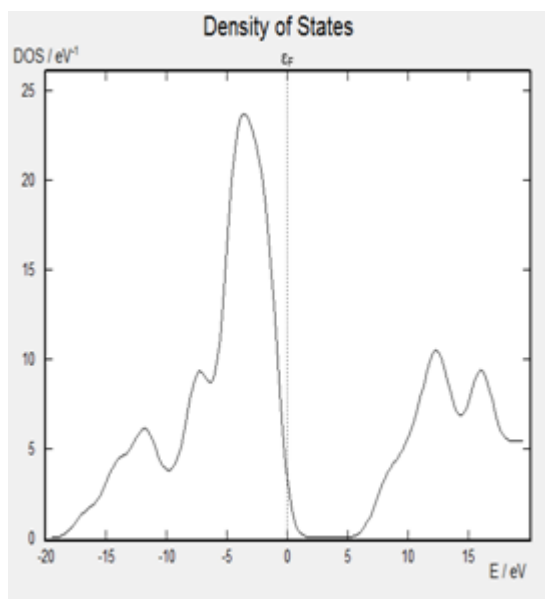
DOS/ev on y axis and 4,9,6,17,20, 25 E/ev in x axis resp. Now this bulk Sillicon nanowire is doped with two P atoms, the graph becomes very dense and it clearly defends very high metallic nature. There are three peaks on both sides of femi level . The peaks appears on 23, 6.2, 9.2 DOS/ev on one side of Fermi level which is at -0.3, -12.5, -21.6 in x axis .But when this Sillicon nanowire is doped with three P atoms, we observe one side of Fermi level has three peaks, the graph shows peaks which is at -1.3,-0.5,-1.7 DOS/ev in y axis and 10.3,10.4,10.2E/ev on x axis resp . But on the other side, there are many small peaks. We observe lot of distorted peaks on the valence band which defends it is metallic .Finally this bulk Sillicon nanowire is doped with four P atoms , the graph shows a three peaks on one side of fermi level which is at 7.5, 12.6,19.8 DOS/ev in y axis and other side has around seven peaks which appears on 9.6 , 10.4 , 4.7 ,5.4,4.8,1.8,1 DOS/ev .Here , we see small peaks raising up .As usual there is presence of more peaks but now the peaks are getting distorted on both sides because of increase in number of electrons of Aluminium and phosphorous atoms .



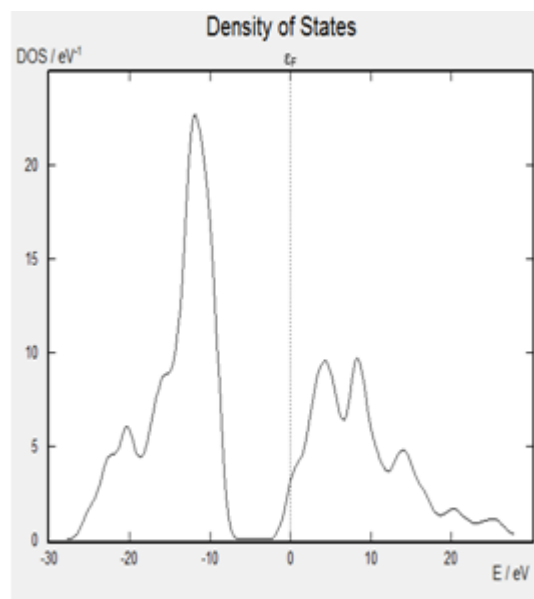


(e)

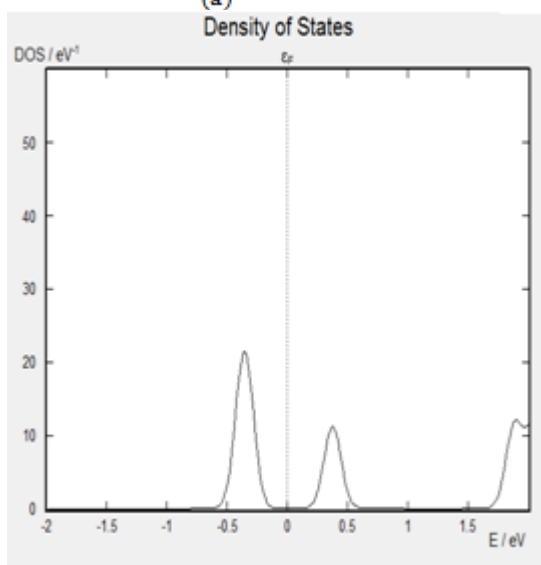
**Figure 6:** The Density of States of Si nanowires (a) SiNW without doping, (b) SiNW doped with 1 Al atom, (c) SiNW doped with 2 Al atoms, (d) SiNW doped with 3 Al atoms and (e) SiNW Doped with 4 Al atoms



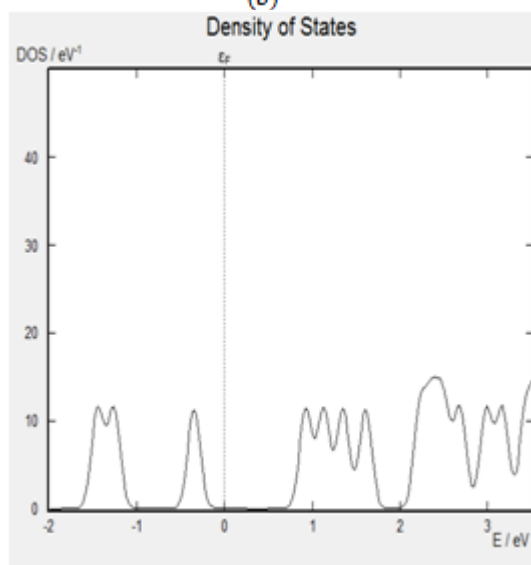
(a)



(b)



(c)



(d)

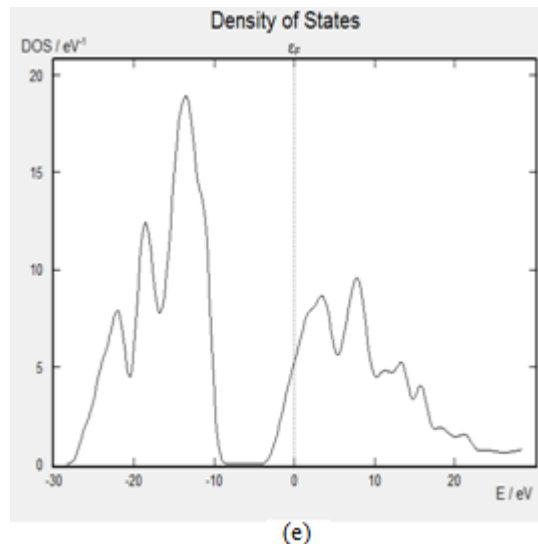


**Figure 7:** The Density of structures of Si nanowires (a) SiNW without doping , (b) SiNW doped with 1 P atom , (c) SiNW doped with 2 P atoms , (d) SiNW doped with 3 P atoms and (e) SiNW Doped with 4 P atoms

#### 4. Conclusions

After analysing the structural and electronics properties of Silicon nanowire, we can conclude that in case of structural property, if total energy is maximum then the structure is least stable. So we can say that total energy is inversely proportional to stability with the increase of doping Al and P atoms, total energy is increasing. In density of states, we clearly see the decline in DOS/Ev with the increase of doping Al and P atoms. But the graph was getting denser and crowded with conduction lines as the metallic property is increasing. Finally , in Bandstructure , we observe that band gap gets hidden because of crowded conduction lines while doping it with Al and P atoms which depicts the increase of metallic nature as earlier in case of Si NW , there was small band gap available depicting semiconductor property.

#### 5. Acknowledgement

Authors greatly acknowledge the support from ABP-IIITM Gwalior for providing the infrastructure support in doing the research work.

#### References

- [1] Volker Schmidt,\* Joerg V. Wittemann, Stephan Senz, and Ulrich Go'sele , Adv. Mater. 2009, 21, 2681–2702
- [2] Mehedhi Hasan<sup>1</sup>, Md Fazlul Huq<sup>2\*</sup> and Zahid Hasan Mahmood , © 2013 Hasan et al.; licensee Springer
- [3] Kui-Qing Peng<sup>a</sup>, Xin Wang<sup>a</sup>, Li Li<sup>a</sup>, Ya Hu<sup>a</sup>, Shuit-Tong Lee , 10.1016/j.nantod.2012.12.009
- [4] F.Patolsky and C.M.Lieber , Mater. Today 8,20(2005)
- [5] A.M.Morales and C.M.Lieber, Science 279,208(1998)
- [6] Bozhi Tian<sup>1,3</sup>, Xiaolin Zheng<sup>1,3</sup>, Thomas J. Kempa<sup>1</sup>, Ying Fang<sup>1</sup>, Nanfang Yu<sup>2</sup>, Guihua Yu<sup>1</sup>, Jinlin Huang<sup>1</sup> & Charles M. Lieber , *Nature* 449, 885-889 (18 October 2007)
- [7] Z.G.Bai,D.P.Yu,J.J.Wang,Y.H.Zou,W.Qian,J.S.Fu,S.Q.Feng,J.Xu and L.P. You , Mater.Sci.Eng.,B 72,117 (2000)
- [8] D.B.Geohegan,A.A.Puretzky , G.Dushcher and S.J. Pennycook , Appl. Phys Lett.73.438
- [9] M. Hofheinz , X.Jehi , M. Sanquer , G.Molas , M.Vinet and S.Deleonibus ,Eur .Phys.J.B 54, 299(2006)
- [10]D.D.D.Ma ,C.S.Lee, F.C.K.Au , S.Y. Tong and S.T.Lee , Science 299 , 1874(2003)
- [11] <http://www.atomistix.com>
- [12]Jeremy Taylor , Hong Guo and Jian Wang ,Phys.Rev.B 63,245407(2001)
- [13]Mads Brandbyge , Jose-Luis Mozos , Pablo Ordejon , Jeremy Taylor and Kurt Stokbro, Phys.Rev. B 65 , 165401 (2002)
- [14]Kurt Stokbro , Jeremy Taylor , Mads Brandbyge and Pablo Ordejon , Annals N.Y.Acad.Sci.1006,212 (2003)
- [15]Jose M. Soler , Emilio Artacho , Julian D.Gale , Alberto Garcia , Javier Junquera , Pablo Ordejon and Daniel Sanchez Portal,J.Phys.Cond.Mat.14,2745(2002)
- [16]B. Hammer , L.B. Hansen and J.K. Norskov , "Improved adsorption energetics within density Functional theory using revised Perdew-Burke-
- [17]Anurag Shrivastav , Neha Tyagi and R.K.Singh , JCTN, Vol.8.1-6,2011
- [18]Anurag Shrivastav , Neha Tyagi and R.K.Singh , Materials Chemistry and Physics 127 (2011)489-494
- [19]Anurag Srivastava,<sup>1</sup> Mohammad Irfan Khan,<sup>1,2</sup> Neha Tyagi,<sup>1</sup> and Purnima Swaroop Khare , Volume 2014 (2014), Article ID 984591